Robust Control of Ill-Conditioned Plants: High-Purity Distillation

SIGURD SKOGESTAD, MANFRED MORARI, MEMBER, IEEE, AND JOHN C. DOYLE

Abstract—Ill-conditioned plants are generally believed to be difficult to control. Using a high-purity distillation column as an example, the physical reason for the poor conditioning and its implications on control system design and performance are explained. It is shown that an acceptable performance/robustness trade-off cannot be obtained by simple loop-shaping techniques (via singular values) and that a good understanding of the model uncertainty is essential for robust control system design. Physically motivated uncertainty descriptions (actuator uncertainty) are translated into the H_∞/structured singular value framework, which is demonstrated to be a powerful tool to analyze and understand the complex phenomena.

I. INTRODUCTION

IT is well known that ill-conditioned plants may cause control problems [1]–[5]. By ill-conditioned we mean that the plant gain is strongly dependent on the input direction, or equivalently that the plant has a high condition number

$$\gamma(G(j\omega)) = \frac{\bar{\sigma}(G(j\omega))}{\underline{\sigma}(G(j\omega))} . \tag{1}$$

Here $\bar{\sigma}(G)$ and $\underline{\sigma}(G)$ denote the maximum and minimum singular values of the plant

$$\bar{\sigma}(G) = \max_{u \neq 0} \frac{\|Gu\|_2}{\|u\|_2} , \quad \underline{\sigma}(G) = \min_{u \neq 0} \frac{\|Gu\|_2}{\|u\|_2} \tag{2}$$

$\|\cdot\|_2$ denotes the usual Euclidean norm. We also say that an ill-conditioned plant is characterized by strong directionality because inputs in directions corresponding to high plant gains are strongly amplified by the plant, while inputs in directions corresponding to low plant gains are not.

The main reason for the control problems associated with ill-conditioned plants is uncertainty. Uncertainty in the plant model may have several origins.

1) There are always parameters in the linear model which are only known approximately.

2) Measurement devices have imperfections. This may give rise to uncertainty on the manipulated *inputs* in distillation columns, since they are usually measured and adjusted in a cascade manner. In other cases, limited valve resolution may cause input uncertainty.

3) At high frequencies even the structure and the model order are unknown, and the uncertainty will exceed 100 percent at some frequency.

4) The parameters in the linear model may vary due to nonlinearities or changes in the operating conditions.

For tight control of ill-conditioned plants the controller should compensate for the strong directionality by applying large input signals in the directions where the plant gain is low; that is, a controller similar to G^{-1} in directionality is desirable. However, because of uncertainty, the direction of the large input may not correspond exactly to the low plant-gain direction, and the amplification of these large input signals may be much larger than expected from the model. This will result in large values of the controlled variables y (Fig. 1), leading to poor performance or even instability.

The concept of directionality is clearly unique to multivariable systems, and extensions of design methods developed for SISO systems are likely to fail for multivariable plants with a high degree of directionality. Furthermore, since the problems with ill-conditioned plants are closely related to how uncertainty affects the particular plant, it is very important to model the uncertainty as precisely as possible. Most multivariable design methods (LQG, LQG/LTR, DNA/INA, IMC, etc.) do not explicitly take uncertainty into account, and these methods will in general not yield acceptable designs for ill-conditioned plants.

A distillation column will be used as an example of an ill-conditioned plant. Here the product compositions are very sensitive to changes in the external flows (high gain in this direction), but quite insensitive to changes in the internal flows (low gain in this direction). In this paper the main emphasis is on the general properties of ill-conditioned plants, rather than the control system design for real distillation columns. We therefore choose to use a very simple model of the column where the condition number as a function of frequency is constant. The use of a more realistic model is discussed by the authors in another paper [6].

The objective of this paper is to demonstrate with a very simple simulation example that ill-conditioned plants are potentially extremely sensitive to plant uncertainty. Secondly, we show that the structured singular value (SSV, usually denoted μ) provides a rigorous framework for analyzing and understanding this behavior. Necessary and sufficient conditions for robust stability and robust performance may be formulated in terms of μ. The frequency domain is used to specify uncertainty and performance. These specifications are given in terms of magnitude bounds on the H_∞-norm $[\sup_\omega \bar{\sigma}(\cdot)]$ of the uncertainty (Δ) and the sensitivity operator $(S = (I + GC)^{-1})$. In this paper the nominal plant model $(\Delta = 0)$ is denoted by G, and the perturbed model when there is uncertainty is given subscript p (i.e., G_p). We will also refer to the complimentary sensitivity operator $H = GC(I + GC)^{-1} = I - S$ and to the input sensitivity $(S_I = (I + CG)^{-1})$ and input complimentary sensitivity $(H_I = I - S_I)$ operators.

II. DISTILLATION COLUMN EXAMPLE

The objective of the distillation column (Fig. 2) is to split the feed F, which is a mixture of a light and a heavy component, into a distillate product D, which contains most of the light component, and a bottom product B, which contains most of the heavy component. The compositions z_F, y_D, and x_B of these streams refer to the mole fractions of the light component. Perfect separation would be obtained with $y_D = 1$ and $x_B = 0$. The
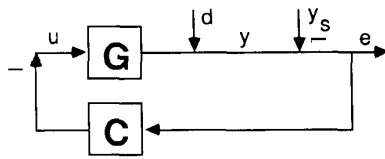
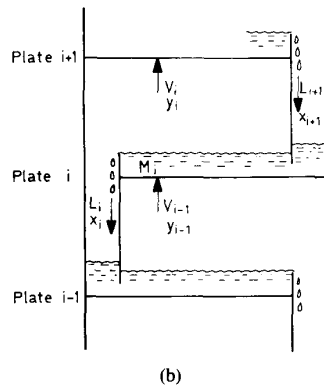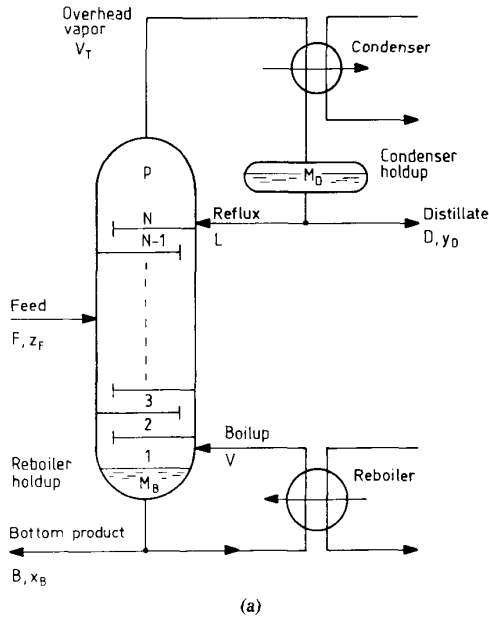Fig. 1.   Classical linear feedback structure.

(a)

(b)

Fig. 2.   Two-product distillation column. Details of the flows and holdups on a plate are shown.

driving force for this separation is the difference in volatility between the light and heavy component. The distillation column in Fig. 2 has five controlled variables:

- vapor holdup (expressed by the pressure p)
- liquid holdup in the accumulator (M_D)
- liquid holdup in the column base (M_B)
- top composition (y_D)
- bottom composition (x_B)

and five manipulated inputs

- distillate flow (D)
- bottom flow (B)
- reflux (L)
- boilup (V) (controlled indirectly by the reboiler duty)

- overhead vapor (V_T) (controlled indirectly by the condenser duty).

Because the composition dynamics are usually much slower than the flow dynamics, we will make the simplifying assumption of perfect control of holdup (i.e., p, M_D, M_B constant) and instantaneous flow responses in the column. Different control *configurations* are obtained by choosing different input pairs (e.g., L and V) for composition control; the remaining three manipulated inputs are then determined by the requirement of keeping p, M_D, and M_B under perfect control. With the additional assumption of constant molar flows this implies that the following three relationships must hold:

$$dV = dV_T, \qquad dD = -dB = dV - dL. \qquad (3)$$

In this paper we will first consider the LV-configuration and then the DV-configuration. Irrespective of the control configuration, the two operating variables corresponding to the high and low plant gain are, as we shall see, the *external* flows and the *internal* flows. The *external* flows are changed by making changes in the product flows B and D (i.e., make a change $dD = -dB$). The *internal* flows are changed by making simultaneous changes in reflux L and boilup V while keeping D and B constant (i.e., make a change $dL = dV$).

Model of the Distillation Column

The distillation column described in Table I will be used as an example. The overhead composition is to be controlled at $y_D = 0.99$ and the bottom composition at $x_B = 0.01$. Consider first using reflux L and boilup V as manipulated inputs for composition control, i.e.,

$$y = \begin{pmatrix} \Delta y_D \\ \Delta x_B \end{pmatrix}, \quad u = \begin{pmatrix} \Delta L \\ \Delta V \end{pmatrix}.$$

This choice is often made since L and V have an immediate effect on the product compositions. By linearizing the steady-state model and assuming that the dynamics may be approximated by a first-order response with time constant $\tau = 75$ min, we derive the following linear model:

$$\begin{pmatrix} dy_D \\ dx_B \end{pmatrix} = G_{LV} \begin{pmatrix} dL \\ dV \end{pmatrix}, \quad G_{LV} = \frac{1}{\tau s + 1} \begin{pmatrix} 0.878 & -0.864 \\ 1.082 & -1.096 \end{pmatrix}. \quad (4)$$

This is admittedly a very crude model of this strongly nonlinear plant, but the model is simple and displays important features of the distillation column behavior.

Singular Value Analysis of the Model

The condition number of the plant (4) is $\gamma(G_{LV}) = 141.7$ which shows a high degree of directionality in the plant. More specific information about this directionality is obtained from the singular value decomposition (SVD) of the steady-state gain matrix

$$G = U \Sigma V^H$$

or equivalently since $V^H = V^{-1}$

$$G\bar{v} = \bar{\sigma}(G)\bar{u}, \quad G\underline{v} = \underline{\sigma}(G)\underline{u}$$

where

$$\Sigma = \text{diag} \{\bar{\sigma}, \underline{\sigma}\} = \text{diag} \{1.972, 0.0139\}$$

$$V = (\bar{v} \ \underline{v}) = \begin{pmatrix} 0.707 & 0.708 \\ -0.708 & 0.707 \end{pmatrix}$$

$$U = (\bar{u} \ \underline{u}) = \begin{pmatrix} 0.625 & 0.781 \\ 0.781 & -0.625 \end{pmatrix}.$$

TABLE I
STEADY-STATE DATA FOR DISTILLATION COLUMN EXAMPLE

Binary separation, constant molar flows, feed liquid.

Column Data:

	Relative Volatility	$\alpha = 1.5$
	No. of theoretical trays	$N = 40$
	Feed tray (1=reboiler)	$N_F = 21$
	Feed composition	$z_F = 0.5$

Operating variables:

$y_D =$	0.99
$x_B =$	0.01
$D/F =$	0.500
$L/F =$	2.706

Steady-state gains :

$$\begin{pmatrix} dy_D \\ dx_B \end{pmatrix} = \begin{pmatrix} 0.878 & -0.864 \\ 1.082 & -1.096 \end{pmatrix} \begin{pmatrix} dL/F \\ dV/F \end{pmatrix}$$

The large plant gain $\bar{\sigma}(G) = 1.972$ is obtained when the inputs are in the direction $\left(\frac{dL}{dV}\right) = \bar{v} = \left(\begin{smallmatrix} 0.707 \\ -0.708 \end{smallmatrix}\right)$. Since $dB = dL - dV$ (3), this physically corresponds to the largest possible change in the *external* flows D and B. From the direction of the output vector $\bar{u} = \left(\begin{smallmatrix} 0.625 \\ 0.781 \end{smallmatrix}\right)$, we see that it causes the outputs to move in the same direction, that is, mainly affects the average composition $(y_D + x_B)$. All columns with both products of high purity are sensitive to changes in the external flows because the product rate D has to be about equal to the amount of light component in the feed. Any imbalance leads to large changes in product compositions [7].

The low plant gain $\underline{\sigma}(G) = 0.0139$ is obtained for inputs in the direct $\left(\frac{dL}{dV}\right) = \underline{v} = \left(\begin{smallmatrix} 0.708 \\ 0.707 \end{smallmatrix}\right)$. From (3) we observe that this physically corresponds to changing the *internal* flows only $(dB = -dD \approx 0)$, and from the output vector $\underline{u} = \left(\begin{smallmatrix} 0.781 \\ -0.625 \end{smallmatrix}\right)$ we see that the effect is to move the outputs in different directions, that is, to change $y_D - x_B$. Thus, it takes a large control action to move the compositions in different directions, that is, to make both products purer simultaneously.

The notion that some changes are more difficult than others is important, since it implies that some disturbances may be easier to reject than others. Let d represent the *effect* of the disturbance on the outputs (Fig. 1), or let d represent a setpoint change. A disturbance d, which has a direction close to $\bar{u}$, is expected to be easy to reject since it corresponds to the high plant gain. Similarly, a disturbance close to $\underline{u}$ in direction is expected to be more difficult. The disturbance condition number $\gamma_d(G)$ gives a more precise measure of how the disturbance is aligned with the plant directions [8]:

$$\gamma_d(G) = \frac{\|G^{-1}d\|_2}{\|d\|_2} \bar{\sigma}(G). \qquad (5)$$

$\gamma_d(G)$ ranges in magnitude between 1 and $\gamma(G)$. A value close to 1 indicates that the disturbance is in the good direction $(\bar{u})$ corresponding to the high plant gain $\bar{\sigma}(G)$. A value close to $\gamma(G)$ indicates that the disturbance is in the bad direction $(\underline{u})$ corresponding to the low plant gain $\underline{\sigma}(G)$. We will consider the following two disturbances (actually setpoint changes) in the simulations

$$y_{s_1} = \begin{pmatrix} 1 \\ 0 \end{pmatrix} \text{ with } \gamma_{d_1}(G) = 110.5$$

$$y_{s_2} = \begin{pmatrix} 0.4 \\ 0.6 \end{pmatrix} \text{ with } \gamma_{d_2}(G) = 12.3.$$

y_{s_1} corresponds to a setpoint change in y_D only, and it represents a change with a large component in the bad direction corresponding to the low plant gain. Setpoint change y_{s_2} is mostly in the good direction corresponding to the high plant gain, and is therefore expected to be easier for the control system to handle.

Linear Closed-Loop Simulations

Linear simulations of the distillation model (4) will now be used to support the following three claims regarding *ill-conditioned* plants.

1) Inverse-based controllers are potentially very sensitive to uncertainty on the inputs.

2) Low condition-number controllers are less sensitive to uncertainty, but the response is strongly dependent on the disturbance direction.

3) Changing the plant may make even an ill-conditioned plant insensitive to input uncertainty.

1) Inverse-Based Controllers are Potentially Very Sensitive to Uncertainty on the Inputs: The inverse-based controller

$$C_1(s) = \frac{k_1}{s} G_{LV}^{-1}(s) = \frac{k_1(1 + 75s)}{s} \begin{pmatrix} 39.942 & -31.487 \\ 39.432 & -31.997 \end{pmatrix},$$

$$k_1 = 0.7 \text{ min}^{-1} \qquad (6)$$

is obtained by the IMC design procedure with a first-order filter [9] or by using a steady-state decoupler plus a PI-controller. In theory, this controller should remove all the directionality of the plant and give rise to a first-order response with time constant 1.43 min. This is indeed confirmed by the simulations in Fig. 3 for the case with no uncertainty. In practice the plant is different from the model and we also show the response when there is 20 percent error (uncertainty) in the *change* of each manipulated input

$$dL = 1.2dL_c, \quad dV = 0.8dV_c. \qquad (7)$$

(dL and dV are the actual changes in the manipulated flow rates, while dL_c and dV_c are the *desired* values as specified by the controller.) It is important to stress that this diagonal input uncertainty, which stems from our inability to know the exact values of the manipulated inputs, is *always* present. Note that the uncertainty is on the *change* in the inputs (flow rates ΔL and ΔV) and not on their absolute values. A 20 percent error is reasonable for process control applications (some reduction may be possible, for example, by use of cascade control using flow measurements, but there will still be uncertainty because of measurement errors). Anyway, the main objective of this paper is to demonstrate the effect of uncertainty, and its exact magnitude is of less importance.

For setpoint change y_{s_1} the simulated response with uncertainty differs drastically from the one predicted by the model, and the response is clearly not acceptable; the response is no longer decoupled, and Δy_D and Δx_B reach a value of about 6 before settling at their desired values of 1 and 0. As expected, the uncertainty has less deteriorating effect for setpoint change y_{s_2}.

There is a simple physical reason for the observed poor response to the setpoint change in y_D. To accomplish this change, which occurs mostly in the bad direction corresponding to the low plant gains, the inverse-based controller generates a *large* change in the internal flow $(dL + dV)$ while trying to keep the changes in the external flows $(dB = -dD = dL - dV)$ very *small*. However, uncertainty with respect to the values of dL and dV makes it impossible to keep their sum large while keeping their difference small—the result is an undesired *large* change in the external flows, which subsequently results in large changes in the product compositions because of the large plant gain in this direction. This sensitivity to input uncertainty may be avoided by controlling D or B directly as shown below.
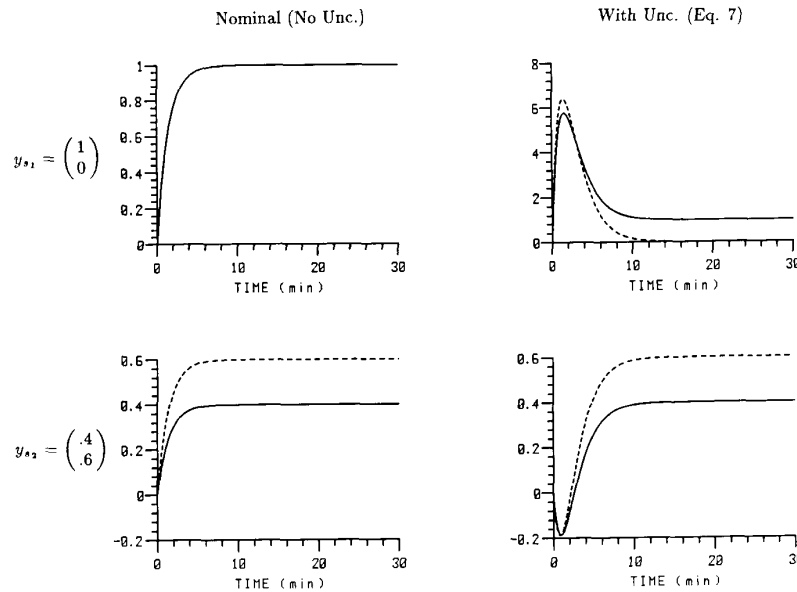
Nominal (No Unc.)   With Unc. (Eq. 7)

Fig. 3. *LV*-configuration. Closed-loop responses Δy_D and Δx_B with inverse-based controller $C_1(s)$, $k_1 = 0.7$.

A more mathematical way of showing how the uncertainty changes the plant is as follows. Let the plant transfer model be $G(s)$ and let Δ_1 and Δ_2 represent the relative uncertainty for each manipulated input. Then the actual (perturbed) plant is

$$G_p = G(I + \Delta_I), \quad \Delta_I = \begin{pmatrix} \Delta_1 & 0 \\ 0 & \Delta_2 \end{pmatrix}.$$

With an inverse-based controller $C(s) = c(s)G(s)^{-1}$, the loop transfer matrix becomes

$$G_p C = c(s)G(I + \Delta_I)G^{-1} = c(s)(I + G\Delta_I G^{-1}). \tag{8}$$

The error term

$$G_{LV}\Delta_I G_{LV}^{-1} = \begin{pmatrix} 35.1\Delta_1 - 34.1\Delta_2 & -27.7\Delta_1 + 27.7\Delta_2 \\ 43.2\Delta_1 - 43.2\Delta_2 & -34.1\Delta_1 + 35.1\Delta_2 \end{pmatrix} \tag{9}$$

is worst when Δ_1 and Δ_2 have different signs. With $\Delta_1 = 0.2$ and $\Delta_2 = -0.2$ [as used in the simulations (7)] we find

$$G_{LV}\Delta_I G_{LV}^{-1} = \begin{pmatrix} 13.8 & -11.1 \\ 17.2 & -13.8 \end{pmatrix}.$$

The elements in this matrix are much larger than one, and the observed poor response is not surprising.

2) Low Condition-Number Controllers are Less Sensitive to Uncertainty, but the Response is Strongly Dependent on the Disturbance Direction: The poor response for the case with uncertainty in the above example was caused by the high condition-number controller which generates large input signals in the direction corresponding to the low plant gain. The simplest way to make the closed-loop system insensitive to input uncertainty is to use a low condition-number controller which does not have large gains in any particular direction. The problem with such a controller is that little or no correction is made for the strong directionality of the plant. This results in a closed-loop response which depends strongly on the disturbance direction. To illustrate this, consider the diagonal controller

$$C_2(s) = \frac{k_2(75s + 1)}{s} \begin{pmatrix} 1 & 0 \\ 0 & -1 \end{pmatrix}, \quad k_2 = 2.4 \text{ min}^{-1} \tag{10}$$

which consists of two equal single-loop PI controllers and has a condition number of one. As seen from the simulations in Fig. 4 the quality of the closed-loop response depends strongly on the disturbance direction, but is only weakly influenced by uncertainty. The response to y_{s_1} is very sluggish, while the response to y_{s_2} is fast initially, but approaches the final steady-state sluggishly. Note that a disturbance entirely in the good direction ($y_s = \bar{u}$) would give a first-order response with time constant $\bar{\sigma}(G)/2.4 = 0.21$ min. On the other hand, a disturbance in the bad direction ($y_s = \underline{u}$) generates a first-order response with time constant $\underline{\sigma}(G)/2.4 = 30$ min. All other responses are linear combinations of these two extremes (Fig. 4).

3) Changing the Plant May Make Even an Ill-Conditioned Plant Insensitive to Input Uncertainty: We already argued physically that the plant might be made less sensitive to uncertainty by controlling the external flows directly. Consider the case of distillate flow D and boilup V as manipulated variables (direct material balance control [7]). Assuming perfect level and pressure control, i.e., $dL = dV - dD$ (3), we have

$$\begin{pmatrix} dL \\ dV \end{pmatrix} = \begin{pmatrix} -1 & 1 \\ 0 & 1 \end{pmatrix} \begin{pmatrix} dD \\ dV \end{pmatrix} \tag{11}$$

and the following linear model is derived from (4):

$$\begin{pmatrix} dy_D \\ dx_B \end{pmatrix} = G_{DV} \begin{pmatrix} dD \\ dV \end{pmatrix}$$

$$G_{DV} = G_{LV} \begin{pmatrix} -1 & 1 \\ 0 & 1 \end{pmatrix} = \frac{1}{1 + 75s} \begin{pmatrix} -0.878 & 0.014 \\ -1.082 & -0.014 \end{pmatrix}. \tag{12}$$

In practice, the condenser level loop introduces a lag between the change in distillate flow dD and the reflux flow dL (which is the input which actually affects the compositions), but this is neglected here. The plant (12) is also ill-conditioned; $\gamma(G_{DV}) = 70.8$. In this case the SVD yields

$$\Sigma = \begin{pmatrix} 1.393 & 0 \\ 0 & 0.0197 \end{pmatrix}, \quad V = \begin{pmatrix} -1.000 & -0.001 \\ -0.001 & 1.000 \end{pmatrix},$$

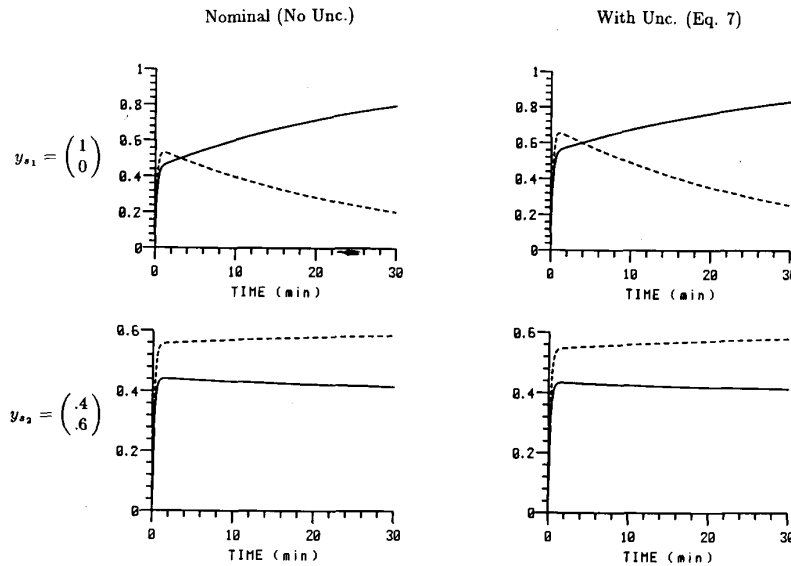$$U = \begin{pmatrix} 0.630 & 0.777 \\ 0.777 & -0.630 \end{pmatrix}.$$

Fig. 4. LV-configuration. Closed-loop responses Δy_D and Δx_B with diagonal controller $C_2(s)$, $k_2 = 2.4$.
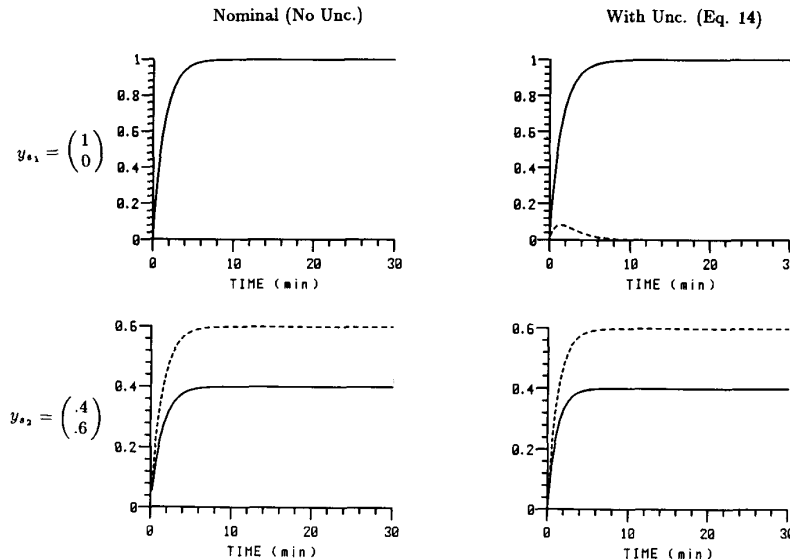

Fig. 5. DV-configuration. Closed-loop responses Δy_D and Δx_B with inverse-based controller $C_3(s)$, $k_3 = 0.7$.

The high gain corresponds to an input $(\frac{dD}{dV})$ in the direction of $\bar{v}(G_{DV}) = \binom{-1.000}{-0.001}$ which, as expected, corresponds to a change in the external flows. The low gain again corresponds to a change in the internal flows $(dD \cong 0)$. Note that in this case there is one manipulated variable (dD) which acts in the high gain direction, and another (dV) which acts in the low gain direction. This decomposition is significant since uncertainty in dV does not affect the external flows dD.

To confirm that the system is much less sensitive to uncertainty in this case, consider the following inverse-based controller:

$$C_3(s) = \frac{k_3}{s} G_{DV}^{-1}(s) = \frac{k_3(1+75s)}{s} \begin{pmatrix} -0.5102 & -0.5102 \\ 39.43 & -32.00 \end{pmatrix},$$

$$k_3 = 0.7 \quad \text{min}^{-1}. \quad (13)$$

Without uncertainty, this controller gives the *same* response as

with $C_1(s)$ applied to the LV-configuration. However, for the DV-configuration the decoupled first-order response with time constant 1.43 min is also maintained when there is 20 percent uncertainty on the manipulated inputs (Fig. 5). The following errors with respect to dD and dV were used:

$$dD = 1.2dD_c, \quad dV = 0.8dV_c. \quad (14)$$

From this example we see that ill-conditioned plants by themselves may not give performance problems provided the uncertainty is appropriately aligned with the plant.

For the DV-configuration we find the error matrix $G\Delta_I G^{-1}$ in (8)

$$G_{DV}\Delta_I G_{DV}^{-1} = \begin{pmatrix} 0.45\Delta_1 + 0.55\Delta_2 & 0.45\Delta_1 - 0.45\Delta_2 \\ 0.55\Delta_1 - 0.55\Delta_2 & 0.55\Delta_1 + 0.45\Delta_2 \end{pmatrix} \quad (15)$$

and with $\Delta_1 = 0.2$ and $\Delta_2 = -0.2$ corresponding to (14)

$$G_{DV}\Delta_I G_{DV}^{-1} = \begin{pmatrix} -0.02 & 0.18 \\ 0.22 & 0.02 \end{pmatrix}.$$

The elements in this matrix are small compared to one, and good performance is maintained even in the presence of uncertainty on each input. The nonzero off-diagonal elements explain why the response to y_{s_1} in the case with uncertainty (upper right in Fig. 5) is not completely decoupled.

III. ROBUSTNESS ANALYSIS WITH μ

It is quite evident from the linear simulations above that multivariable systems exhibit a type of directionality which makes the closed-loop response strongly dependent on the particular disturbance and model error assumed. One of the major weaknesses with the simulation approach is that it may be very difficult and time-consuming to find the particular input signal and model error which causes control problems. Therefore, there is a need for a tool which solves the following problem in a systematic manner.

Robust Performance Problem: Given a nominal plant model, an uncertainty description, a set of possible external input signals (disturbances, setpoints), a desired performance objective, and a controller: Will the worst case response satisfy the desired performance objective? As we will show, the structured singular value μ proves to be a useful tool for solving this problem. A definition of μ with some of its properties is given in the Appendix.

Achieving robust performance is clearly the ultimate goal for the controller design. However, it may be easier to solve this problem by first considering the following subobjectives which have to be satisfied in order to achieve robust performance.

Nominal Stability (NS): The closed-loop system with the controller applied to the (nominal) plant model must be stable.

Nominal Performance (NP): In addition to stability, the quality of the response should satisfy some minimum requirement. We will define performance in terms of the weighted H_∞-norm of the closed-loop transfer function between external inputs (disturbances and setpoints) and errors (may include $y - y_s$, manipulated inputs u, etc.) The simplest example of such a performance specification is a bound on the weighted sensitivity operator

$$NP \Leftrightarrow \bar{\sigma}(W_{1P}SW_{2P}) < 1 \quad \forall\omega. \tag{16a}$$

The input weight W_{2P} is often equal to the disturbance model. The output weight W_{1P} is used to specify the frequency range over which the errors are to be small and (if W_{1P} is not equal to $w_P I$) which outputs are more important.

Robust Stability (RS): The closed-loop system must remain stable for all possible perturbed plants (G_p) as defined by the uncertainty description.

Robust Performance (RP): The closed-loop system must satisfy the performance specifications for all possible plants. As an example we may require (16a) to be satisfied when G is replaced by any of the possible G_p

$$RP \Leftrightarrow \bar{\sigma}(W_{1P}S_pW_{2P}) < 1 \quad \forall\omega, \ \forall G_p \tag{16b}$$

where $S_p = (I + G_pC)^{-1}$.

The stability margins of the classical frequency domain design methods are an attempt to address the robust stability problem, but the margins may be misleading and are a very indirect method.

The definitions above for robust stability and robust performance are of no value without simple tests that may be used to tell, for example, whether (16b) is satisfied for all possible plants G_p. Below we state practical (computationally useful) conditions for RS and RP using the structured singular value of μ.
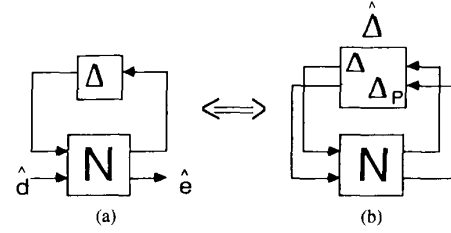

Fig. 6. General representation of system with uncertainty Δ. Robust performance (19) of (a) is equivalent to robust stability of (b).

Interconnection Matrix N

To use μ, the uncertainty (i.e., the set of possible plants) must be modeled in terms of norm-bounded perturbations on the nominal system. By use of weights each perturbation is normalized to have magnitude one: $\bar{\sigma}(\Delta_i) \leq 1$, $\forall\omega$. The perturbations, which may occur at different locations in the system, are collected in the *diagonal* matrix

$$\Delta = \text{diag}\{\Delta_1, \cdots, \Delta_n\}, \ \bar{\sigma}(\Delta) \leq 1, \ \forall\omega \tag{17}$$

and the system is rearranged to match the structure of Fig. 6(a). The signals $\hat{d}$ in Fig. 6(a) represent the weighted external inputs (disturbances and setpoints) to the system. The signals $\hat{e}$ represent the weighted errors, or more generally all signals we want to keep small (e.g., $y - y_s$, manipulated inputs u). The interconnection matrix N in Fig. 6 is a function of the nominal plant model G, the controller C, and the uncertainty weights. Performance weights are also absorbed into N in order to normalize the performance specifications involving $\hat{d}$ and $\hat{e}$

$$RP \Leftrightarrow \bar{\sigma}(E) < 1 \quad \forall\omega, \ \forall\Delta \tag{18a}$$

where

$$\hat{e} = E\hat{d}, \quad E = N_{22} + N_{21}\Delta(I - N_{11}\Delta)^{-1}N_{12}. \tag{18b}$$

An example of such a performance specification is (16b). An equivalent statement of the RP-specification (18) is

$$RP \Leftrightarrow \|\hat{e}(j\omega)\|_2 / \|\hat{d}(j\omega)\|_2 < 1 \quad \forall\omega, \ \forall\Delta, \ \forall\hat{d}. \tag{19}$$

This is, the worst case amplification $\|\hat{e}\|_2 / \|\hat{d}\|_2$ for any direction of $\hat{d}$, for any frequency ω, and for any model error Δ, must be less than one.

Practical Conditions for Robust Stability

Nominal stability ($\Delta = 0$) is achieved when the interconnection matrix N is stable. The uncertainty (perturbations, Δ) creates additional feedback paths and may therefore give rise to stability problems. Consider the closed-loop transfer function E (18b) from $\hat{d}$ to $\hat{e}$. Since N and Δ are assumed stable, instability can only occur if $(I - N_{11}\Delta)^{-1}$ is unstable [10]. The system is therefore stable if and only if det $(I - N_{11}\Delta)$ does not encircle the origin as s traverses the Nyquist D contour for all possible Δ's. Because the perturbations Δ are norm-bounded (i.e., *all* Δ's satisfying $\bar{\sigma}(\Delta) \leq 1$, $\forall\omega$, are allowed) this is equivalent to [10]

$$\det (I - N_{11}\Delta) \neq 0, \ \forall\omega, \ \forall\Delta, \ \bar{\sigma}(\Delta) \leq 1. \tag{20}$$

Condition (20) is by itself not useful since it is only a yes/no condition which must be tested for all possible Δ's. What is desired is a condition on the matrix N_{11}, preferable on some norm of N_{11}. This is achieved by using the structured singular value. The RS-condition (20) is equivalent to ([10], also see the Appendix)

$$\mu_\Delta(N_{11})\bar{\sigma}(\Delta) < 1, \ \forall\omega, \ \forall\Delta, \ \bar{\sigma}(\Delta) \leq 1 \tag{21}$$

which is equivalent to

$$\mu_\Delta(N_{11}) < 1, \quad \forall \omega. \tag{22}$$

Note that (21) may be interpreted as a generalized small gain theorem applied to the closed loop consisting of the blocks N_{11} and Δ.

Practical Conditions for Robust Performance

Nominally ($\Delta = 0$) we have $E = N_{22}$ and nominal performance is achieved when $\bar{\sigma}(N_{22}) < 1$, $\forall \omega$. To achieve robust performance, $\bar{\sigma}(E) < 1$ (18) must be satisfied for all possible Δ's. However, note that since we have used the same norm (H_∞) to bound both the uncertainty and performance, the robust *performance*-condition (18) is equivalent to requiring robust *stability* of the system N [Fig. 6(b)] subject to the large perturbation $\hat{\Delta} = \text{diag}\{\Delta, \Delta_P\}$. The fictitious perturbation block Δ_P, which is a full matrix of the same size as E and N_{22}, ensures that the performance specification (18) is satisfied. (Note that $\bar{\sigma}(E) = \mu_{\Delta_P}(E)$, see (A-1) and (A-2) in the Appendix.) Consequently, RP is achieved if and only if $\mu_{\hat{\Delta}}(N) < 1$, $\forall \omega$ [10].

Summary of μ-Conditions for RS, NP, and RP

With the above assumptions for the uncertainty (17) and performance (18) we have the following results [10]:

$$NS \Leftrightarrow N \text{ stable (internally)} \tag{23a}$$

$$NP \Leftrightarrow \mu_{NP} = \sup_\omega \bar{\sigma}(N_{22}) < 1 \tag{23b}$$

$$RS \Leftrightarrow \mu_{RS} = \sup_\omega \mu_\Delta(N_{11}) < 1 \tag{23c}$$

$$RP \Leftrightarrow \mu_{RP} = \sup_\omega \mu_{\hat{\Delta}}(N) < 1 \tag{23d}$$

where $\hat{\Delta} = \text{diag}\{\Delta, \Delta_P\}$. The quantities μ_{NP}, μ_{RS}, and μ_{RP} represent the μ-"norms" and are introduced as a convenient notation. Note that the conditions for NP and RS are necessary in order to satisfy the RP-condition.

IV. μ-ANALYSIS OF THE COLUMN

Problem Definition

To study robust stability and robust performance of the distillation column with μ, the uncertainty and performance specifications must first be defined. The same uncertainty and performance specifications will be assumed for the LV-configuration (4) and the DV-configuration (12). (In general, it is reasonable to use the same performance specifications, but the uncertainty may be different.)

Uncertainty: The uncertainty with respect to the manipulated inputs that was used in the simulations in Section II may be represented as multiplicative input uncertainty (Fig. 7)

$$G_p = G(I + w_I(s)\Delta_I), \quad \bar{\sigma}(\Delta_I) < 1 \quad \forall \omega \tag{24}$$

where $w_I(s)$ gives the magnitude of the relative uncertainty on each manipulated input. We choose the following weight:

$$w_I(s) = 0.2 \frac{5s + 1}{0.5s + 1}. \tag{25}$$

This implies an input error of up to 20 percent in the low frequency range as was used in the simulations. The uncertainty increases at high frequency; reaching a value one (100 percent) at about $\omega = 1 \text{ min}^{-1}$. This increase may take care of neglected flow
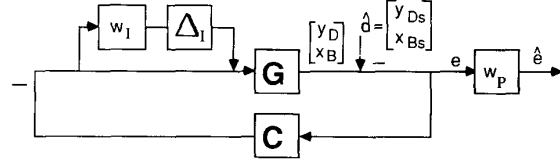

Fig. 7. Block diagram of plant with input uncertainty and with setpoints as external inputs. Rearranging this system to match Fig. 6 gives N as in (28).

dynamics. For example, it allows for a time delay of about 1 min in the responses between L and V and the outputs y_D and x_B. At first the uncertainty will be assumed to be *unstructured;* that is, the perturbation matrix Δ_I is a *full* 2×2 matrix. The off-diagonal terms allowed in Δ_I imply that a change in the one input may result in an undesired change in the other one. This may be the case for some plants, for example, if the actuators are located very close to each other. However, for most plants, including our distillation column, it is more reasonable to assume that the actuators are *independent*, that is, Δ_I is diagonal. However, for mathematical convenience we will assume for now that Δ_I is a full matrix. It happens that this assumption does not make any difference for the LV-configuration.

Performance: We use $\hat{d} = y_s$ as external inputs and $\hat{e} = w_P(y - y_s)$ as weighted errors (Fig. 7) and choose the performance weight

$$w_P(s) = 0.5 \frac{10s + 1}{10s}. \tag{26}$$

The RP-specification (16b) then becomes

$$RP \Leftrightarrow \bar{\sigma}(S_p) < 1/|w_P|, \quad \forall \omega, \forall G_p. \tag{27}$$

The performance weight $w_P(s)$ (26) implies that we require integral action at low frequency ($w_P(0) = \infty$) and allow an amplification of disturbances at high frequencies by at most a factor of two ($|w_P(j\infty)|^{-1} = 2$). A particular sensitivity function which exactly matches the performance bound (27) at low frequencies and satisfies it easily at high frequencies is $S = (20s/20s + 1)I$. This corresponds to a first-order response with time constant 20 min.

Performance and Stability Conditions

With the information given above the matrix N in the ΔN-structure (Fig. 6) becomes

$$N = \begin{pmatrix} -w_I CSG & w_I CS \\ w_P SG & -w_P S \end{pmatrix}. \tag{28}$$

This matrix is found from Fig. 7 by breaking the loops ($\Delta_I = 0$) at the input and output of the block Δ_I. As an example, with $\Delta_I = 0$, the transfer function from the external inputs ($\hat{d}$) to the errors ($\hat{e}$) is $N_{22} = -w_P(I + GC)^{-1}$. Similarly, the transfer function from $\hat{d}$ to the input of Δ_I is $N_{12} = w_I C(I + GC)^{-1}$. Conditions for NP and RS are derived from (28) by using (23b) and (23c)

$$NP \Leftrightarrow \bar{\sigma}(S) < 1/|w_P| \quad \forall \omega \tag{29}$$

$$RS \Leftrightarrow \bar{\sigma}(H_I) < 1/|w_I|, \quad \forall \omega. \tag{30}$$

(The condition for RS is expressed in terms of the singular value $\bar{\sigma}$ since Δ_I is assumed to be a full matrix.) Note that S is the nominal sensitivity operator at the *output* of the plant, while H_I is the complementary sensitivity operator as seen from the *input* of the plant. The RP-specification (27) is tested by computing μ of the matrix N in (28)

$$RP \Leftrightarrow \mu_{\hat{\Delta}}(N) < 1, \quad \forall \omega \tag{31}$$

where $\hat{\Delta} = \text{diag}\{\Delta_I, \Delta_P\}$ and where Δ_I and Δ_P in this case are both full 2×2 matrices.

Simple RP-Conditions for Input Uncertainty

For the case with input uncertainty, the following sufficient (conservative) tests for robust performance (27) in terms of singular values apply:

$$RP \Leftarrow \gamma \cdot \bar{\sigma}(w_P S_I) + \bar{\sigma}(w_I H_I) \le 1, \quad \forall \omega \qquad (32a)$$

or

$$RP \Leftarrow \bar{\sigma}(w_P S) + \gamma \cdot \bar{\sigma}(w_I H) \le 1, \quad \forall \omega \qquad (32b)$$

or

$$RP \Leftarrow (1 + \sqrt{\gamma}) \cdot (\bar{\sigma}(w_P S) + \bar{\sigma}(w_I H_I)) \le 1, \quad \forall \omega. \qquad (32c)$$

Here γ denotes the condition number of the plant *or* the controller (the smallest one should be used). The conditions apply to both diagonal and full block input uncertainty, but are obviously tighter (less conservative) in the latter case. Equations (32a) and (32b) are derived from the *RP*-definition (27) by introducing relationships such as $S_p = S(I + G\Delta_I G^{-1}H)^{-1}$. Equation (32c) is derived from the μ-condition (31) by employing the upper bound $\sup_D \bar{\sigma}(DND^{-1})$ on $\mu(N)$ (A-1)–(A-4).

Conditions (32) indicate that the use of an ill-conditioned controller (i.e., $\gamma(C)$ is large) may give very poor robust performance even though both the nominal performance condition, $\bar{\sigma}(w_P S) < 1$ (29), and robust stability condition, $\bar{\sigma}(w_I H_I) < 1$ (30), are individually satisfied. If a controller with a low condition number (e.g., a diagonal controller with $\gamma(C) = 1$) is used, then we see from (32) that we get *RP* for free provided we have satisfied *NP* and *RS*. This is always the case for SISO systems (which have $\gamma = 1$), and gives a partial explanation for why robust performance was never an important issue in the classical control literature. Furthermore, note that for SISO systems (32a) [or (32b)] is necessary and sufficient for *RP*.

Conditions (32) are useful since they directly relate robust performance to *NP*, *RS* and the condition number. However, (32) may be very conservative and in order to get a tight condition for *RP* the μ-condition (31) has to be used.

Analysis of the LV-Configuration

We will analyze the *LV*-configuration for the inverse-based and the diagonal controller used in the simulations

$$C_1(s) = c_1(s) G_{LV}^{-1}(s), \quad c_1(s) = \frac{k_1}{s} \qquad (33)$$

$$C_2(s) = c_2(s) \begin{pmatrix} 1 & 0 \\ 0 & -1 \end{pmatrix}, \quad c_2(s) = \frac{k_2(1 + 75s)}{s}. \qquad (34)$$

We will first consider the choices $k_1 = 0.7$ and $k_2 = 2.4$ used in the simulations and then see if robust performance can be improved with other choices for k_1 and k_2. Finally, we will consider the μ-optimal controller $C_\mu(s)$, which is obtained by minimizing μ_{RP} in (23d) employing the μ-synthesis procedure of Doyle [11].

Nominal Performance and Robust Stability: One way of designing controllers to meet the *NP* and *RS* specifications is to use multivariable loop-shaping [12]. For *NP*, $\underline{\sigma}(GC)$ must be above $|w_P|$ at low frequencies. For *RS* with input uncertainty, $\bar{\sigma}(CG)$ must lie below $1/|w_I|$ at high frequencies (Fig. 8). For the inverse-based controller (33) we get $\bar{\sigma}(C_1 G) = \sigma(GC_1) = |c_1|$ and it is trivial to choose a $c_1(s)$ which satisfies these conditions. The choice $c_1(s) = 0.7/s$ used in the simulations gives a controller which has much better nominal performance than
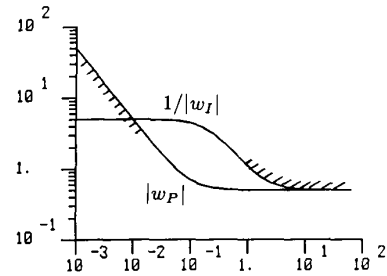

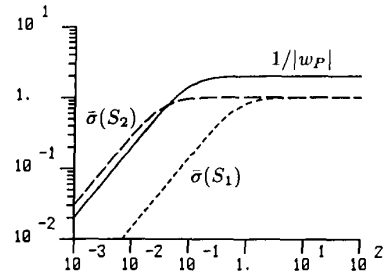Fig. 8. Multivariable loop shaping.
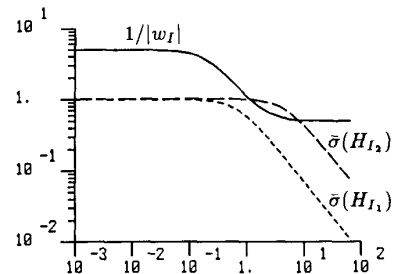

Fig. 9. *LV*-configuration. *NP* bounds.

Fig. 10. *LV*-configuration. *RS* bounds.

required, and which can allow about two times more uncertainty than assumed without becoming unstable. This is also seen from Figs. 9 and 10 where the *NP*- and *RS*-condition (29) and (30) are displayed graphically. For the diagonal controller (34) we find $\bar{\sigma}(C_2 G) = 1.972|c_2|$ and $\sigma(GC_2) = 0.0139|c_2|$, and the difference between these two singular values is so large that no choice of c_2 is able to satisfy both *NP* and *RS* (see Figs. 9 and 10).

Robust Performance: μ for *RP* is plotted in Figs. 11 and 12 for the two controllers used in the simulations. The inverse-based controller $C_1(s)$ is far from satisfying the *RP*-requirements (μ_{RP} is about 5.8), even though the controller was shown to achieve both *NP* and *RP*. This is as expected both from the simulations and from the simple *RP*-bounds (32) (the condition number of the controller $\gamma(C_1)$ is 141.7). On the other hand, the performance of the diagonal controller $C_2(s)$ is much less affected by the uncertainty and we find $\mu_{RP} = 1.70$ in this case. This is also as expected from (32) since $\gamma(C_2) = 1$.

Optimizing k_1 and k_2 with Respect to RP: For the inverse-based controller the optimal value for k_1 is 0.14 corresponding to a value of μ_{RP} equal to 3.3 which still implies poor robust performance. Consequently, it is not possible to achieve acceptable robust performance for this plant with this controller structure.

For the diagonal PI-controller, the optimal gain is $k_2 = 2.4$, which is the value already used. It is not clear how low μ_{RP} can be made if $C(s)$ is only restricted to be diagonal (decentralized control); we were able to get μ_{RP} down to 1.34 by employing two PID controllers with a total of six adjustable parameters.
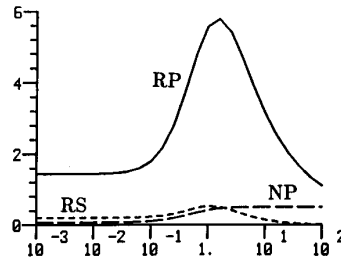
Fig. 11. LV-configuration. μ-plots for inverse-based controller $C_1(s)$, $k_1 =$ 0.7
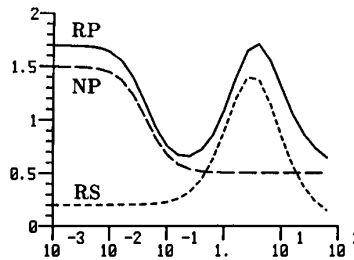

Fig. 12. LV-configuration. μ-plots for diagonal controller $C_2(s)$, $k_2 = 2.4$.

TABLE II
STATE-SPACE REALIZATION OF μ-OPTIMAL CONTROLLER $C_\mu(s) = C(sI - A)B^{-1} + D$

$$A = \begin{pmatrix} -1.002 \cdot 10^{-7} & 0 & 0 & 0 & 0 & \\ 0 & -3.272 \cdot 10^{-6} & 0 & 0 & 0 & 0 \\ 0 & 0 & -0.1510 & 0 & 0 & 0 \\ 0 & 0 & 0 & -9.032 & 0 & 0 \\ 0 & 0 & 0 & 0 & -538.2 & 0 \\ 0 & 0 & 0 & 0 & 0 & -586.8 \end{pmatrix} \qquad B = \begin{pmatrix} -65.13 & -90.09 \\ 72.24 & 90.31 \\ 5.492 & -4.394 \\ -90.86 & -113.6 \\ 1867 & -1494 \\ 672.2 & 840.3 \end{pmatrix}$$

$$C = \begin{pmatrix} 0.6564 & 0.7171 & 4.949 & 5.033 & -1691 & -311.2 \\ 0.6555 & 0.5425 & 4.941 & -5.040 & -1689 & 311.6 \end{pmatrix} \qquad D = \begin{pmatrix} 5866 & -3816 \\ 5002 & -4878 \end{pmatrix}$$

μ-*Optimal Controller:* We found the μ-optimal controller through a software package which uses a somewhat simplified version of the μ-synthesis procedure described by Doyle [11]. The simplification involves only considering the upper left corner when minimizing the H_∞-norm of (7.3) in Doyle's paper [11]. This means that the resulting controller is not quite optimal. The synthesis procedure yields controllers of very high order, but by employing model reduction we were able to find the sixth-order μ-optimal controller given in Table II. At low frequency the controller is approximately

$$C_\mu = \frac{(1+75s)}{s} \begin{pmatrix} 3.82 & -0.92 \\ 1.73 & -3.52 \end{pmatrix} \quad \text{for } \omega \leq 0.1. \quad (35)$$

The condition number at low frequency is 2.1, which means that the controller provides some compensation for the directionality of the plant ($\gamma(G(0)) = 141.7$, while $\gamma(GC_\mu(0)) = \gamma(C_\mu G(0)) = 66.5$). μ for RP for the controller $C_\mu(s)$ has a peak value of 1.06 (Fig. 13), which means that this controller almost satisfies the robust performance condition. This value for μ_{RP} is significantly lower than that for the diagonal PI controller, and the time response is also better as seen from Fig. 14. In particular, the approach to steady state is much faster.

Structure of Δ_I: Note that Δ_I was assumed a full matrix in all the above calculations. It turns out that for this particular plant (4), the same values are found for μ_{RS} and μ_{RP} also when Δ_I is assumed diagonal which is a more reasonable assumption from physical

considerations [recall the discussion that follows (25)]. On the other hand, for the DV-configuration below it is crucial that Δ_I is modeled as a diagonal and not as a full matrix.

Analysis of the DV-Configuration

The set of possible plants is given by (24) with $G = G_{DV}$ (12), and with Δ_I restricted to diagonal. We will consider an inverse-based and a diagonal PI controller

$$C_3(s) = \frac{k_3}{s} G_{DV}^{-1}(s) \quad (13)$$

$$C_4(s) = \frac{(1+75s)}{s} \begin{pmatrix} -0.15 & 0 \\ 0 & -7.5 \end{pmatrix}. \quad (36)$$

In the simulations in Section II we studied the controller $C_3(s)$ with $k_3 = 0.7$. For this controller the NP- and RS-conditions are identical to those of the controller $C_1(s)$ with the LV-configuration. However, based on the simulations and other arguments presented before, we expect μ for robust performance to be much better for the DV-configuration. This is indeed confirmed by the μ-plots in Fig. 15. μ_{RP} is 0.95 which means that the performance criterion is satisfied for all possible model errors. (Note that the condition number of both the plant and controller is 70.8, and the simple singular-value tests (32) prove to be extremely conservative in this case.) The uncertainty block Δ_I was assumed diagonal
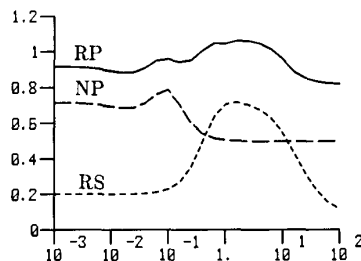
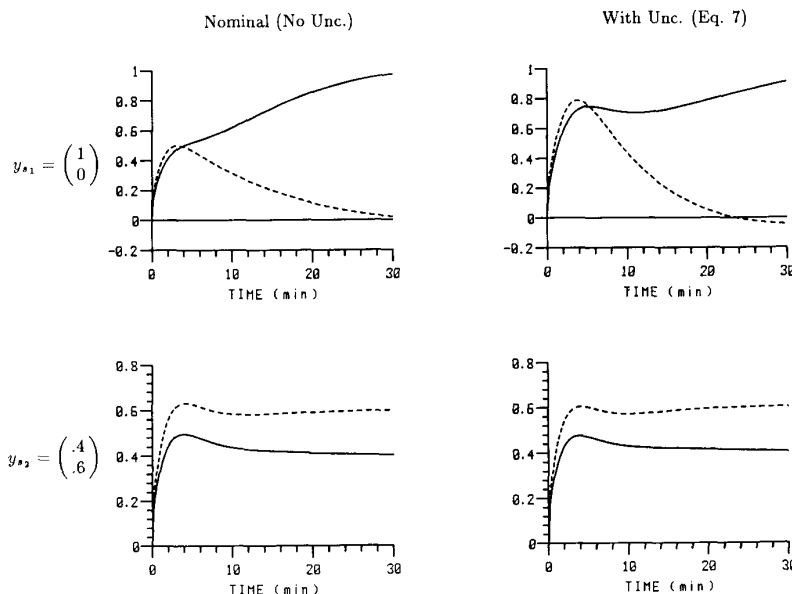Fig. 13. LV-configuration. μ-plots for μ-optimal controller $C_\mu(s)$.

Nominal (No Unc.)   With Unc. (Eq. 7)

$$y_{s_1} = \begin{pmatrix} 1 \\ 0 \end{pmatrix}$$

$$y_{s_2} = \begin{pmatrix} .4 \\ .6 \end{pmatrix}$$

Fig. 14. LV-configuration. Closed-loop responses Δy_D and Δx_B with μ-optimal controller $C_\mu(s)$.
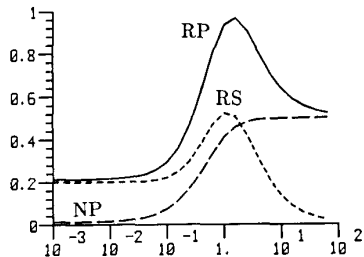

Fig. 15. DV-configuration. μ-plots for inverse-based controller $C_3(s)$, $k_3 =$ 0.7.

when computing μ. If Δ_I were full (which is not the case) the value of μ_{RP} would be about 4.1. The reason for this high value is that off-diagonal elements in Δ_I introduce errors in D when V is changed.

Even lower values for μ are obtained by reducing k_3 from 0.7 to 0.13 which yields $\mu_{RP} = 0.63$. In fact, this controller seems to be close to μ-optimal as we were not able to reduce μ_{RP} below this value.

With $C_4(s)$, which consists of two PI-controllers, $\mu_{RP} = 1.15$. This is almost acceptable, although the value of μ_{RP} is significantly higher than for the inversed-based controller $C_3(s)$ with $k_3 = 0.13$. Thus, a decentralized controller gives acceptable performance.

The potential conservativeness in using $\bar{\sigma}$ instead of μ is clearly illustrated by considering the robust stability test for this case (Fig. 16). Using $\mu_{\Delta_I}(H_I)$ (Δ_I diagonal) we see that the system satisfies the RS condition. However, by looking at $\bar{\sigma}(H_I)$ (or equivalently by computing μ with Δ_I a full matrix), we would erroneously expect the system to become unstable for very small errors on the inputs.

V. UNCERTAINTY MODELING

In this section we will first discuss in somewhat general terms how to quantify uncertainty and then consider as an example other sources than input uncertainty for the distillation column. In order to use the framework for analyzing systems with uncertainty outlined in Section III, we need to model the uncertainty as norm bounded perturbations. Since the uncertainty structure is very problem dependent, it is difficult to give general methods for how to do this. However, the examples given below for the distillation column should be sufficient to show that most uncertainties occurring in practice can be modeled as norm bounded perturbations.

Choosing the Right Structure

It may be very important that the correct structure is chosen for the uncertainty description, i.e., that the uncertainty is modeled as it occurs physically. We will illustrate this by considering the
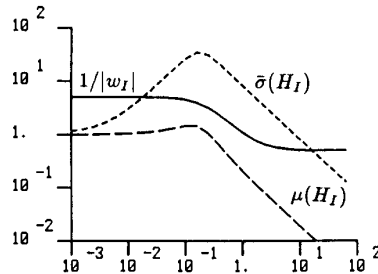
Fig. 16. DV-configuration. RS-bound in terms of singular values ($\bar{\sigma}$) and structured singular values (μ) with controller $C_\mu(s)$.
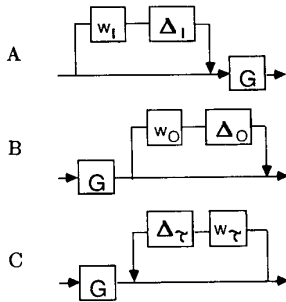

Fig. 17. Three common uncertainty representations.

following two examples:

- multiplicative uncertainty at the input [Fig. 17(a)] or at the output of the plant [Fig. 17(b)];
- output uncertainty as multiplicative [Fig. 17(b)] or inverse multiplicative uncertainty [Fig. 17(c)].

Choices of Multiplicative Uncertainty

The distillation column (as does any plant) has multiplicative uncertainty at the input of the plant. Simply shifting this uncertainty to the output of the plant (and using $w_O = w_I$) will, in general, give a completely different system. As an example, for the LV-configuration using controller $C_1(s)$ we found $\mu_{RP} = 5.78$ with the uncertainty at the input of the plant, but μ_{RP} is only 0.96 if this uncertainty is shifted to the output. Recall condition (32) which showed that with input uncertainty and an ill-conditioned controller, robust performance might be poor even when the RS and NP conditions are satisfied individually. We do not have this problem when the uncertainty is at the output. In this case we get a RP condition similar to (32) but without the condition number

$$RP \iff \bar{\sigma}(w_P S) + \bar{\sigma}(w_O H) \le 1 \quad \forall \omega.$$

This illustrates that output uncertainty usually puts much less constraints on the design of the controller than input uncertainty, and for ill-conditioned plants one should be careful to model the uncertainty at the location where it is actually occurring.

Choices of Output Uncertainty: We will show below that parametric uncertainty in the time constant may be represented as inverse multiplicative uncertainty

$$(I + w_\tau \Delta_\tau)^{-1} G. \tag{37}$$

Approximating it as the seemingly similar multiplicative uncertainty

$$(I + w_O \Delta_O) G \tag{38}$$

has drastically different implications. For robust stability, (37)

imposes a constraint on the sensitivity operator

$$\mu(S) < 1/|w_\tau| \tag{39}$$

and (38) on the complementary sensitivity operator

$$\mu(H) < 1/|w_O|. \tag{40}$$

Equation (37) is best suited to describe pole variations while (38) is better for the modeling of zero variations. Equation (37) cannot be used to describe uncertain high frequency dynamics. Equation (38) cannot be used to model plants which have poles that can cross the $j\omega$-axis.

Simplify If Possible: The two examples above illustrated that it may be very important to model the uncertainties as they occur physically. However, this is not always of crucial importance, and whenever possible the uncertainty description should be simplified by lumping various uncertainties into a single perturbation. There are two reasons for this: 1) computations are simpler; 2) introducing too many sources of uncertainty may be very conservative since it becomes very unlikely for the worst case to occur in practice. In particular, the individual uncertainties may be correlated, and it may be impossible for the worst case to occur. This is illustrated for the distillation column gains below.

Additional Sources of Uncertainty for the Distillation Column

In the following we will consider two additional sources of uncertainty for the distillation column: gain uncertainty and time constant uncertainty (Fig. 18). Physically, these uncertainties may stem from variations in the operating conditions (nonlinearities) which yield parameter variations in the linear model. Treating nonlinearity as uncertainty on a linear model is by no means a rigorous way of handling nonlinearity. However, since it is *not* an objective of this paper to provide an accurate uncertainty description for the distillation column, we will not concern ourselves with these issues. Our objective is to demonstrate how different sources of uncertainty can be modeled as norm-bounded perturbations and fit into the framework in Fig. 6.

All the developments below are for the LV-configuration. However, because of (11) they also apply to the DV-configuration.

Time Constant Uncertainty: Let r_τ represent the magnitude of relative uncertainty on the time constant for each output (y_D and x_B). Then we have the perturbed plant.

$$G_p(s) = \begin{pmatrix} \dfrac{1}{1 + \tau_D s} & 0 \\ 0 & \dfrac{1}{1 + \tau_B s} \end{pmatrix} G(0) \tag{41a}$$

$$\tau_D = \tau(1 + r_\tau \Delta_{\tau D}), \quad |\Delta_{\tau D}| < 1 \quad \forall \omega \tag{41b}$$

$$\tau_B = \tau(1 + r_\tau \Delta_{\tau B}), \quad |\Delta_{\tau B}| < 1 \quad \forall \omega \tag{41c}$$

with $\tau = 75$ min. We will choose $r_\tau = 0.35$, corresponding to 35 percent time constant uncertainty. The scalars $\Delta_{\tau D}$ and $\Delta_{\tau B}$ are independent which allows for different values of τ_D and τ_B. This pole uncertainty may be written in terms of an inverse multiplicative uncertainty at the *output* of the plant as shown in Fig. 18. It is fortunate that it occurs at the output since we know that the system is less sensitive to uncertainty at the output than at the input of the plant. Also note that this kind of inverse output uncertainty puts a constraint on the sensitivity function S, similar to a performance equivalent requirement. The robust stability test for this uncertainty *alone* is

$$\mu_{\Delta_\tau}(S) < 1/|w_\tau|, \quad w_\tau(s) = r_\tau \frac{\tau s}{\tau s + 1} \tag{42}$$

where Δ_τ is a diagonal 2×2 matrix. Clearly, we need $r_\tau < 1$ to satisfy this bound.
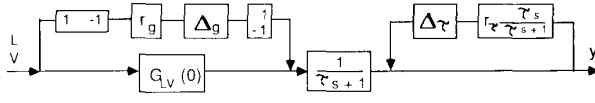
Fig. 18. Block diagram representation of gain uncertainty and time constant uncertainty for distillation column example.

Effect of Additional Uncertainty on μ_{RS} and μ_{RP}: With the time constant uncertainty (41) in addition to the input uncertainty the interconnection matrix N becomes

$$N = \begin{pmatrix} -w_I CSG & -w_I CS & w_I CS \\ w_\tau SG & w_\tau S & w_\tau (I-S) \\ w_P SG & w_P S & -w_P S \end{pmatrix} \qquad (43)$$

$\mu(N)$ for *RP* (Table III) is computed with respect to the structure diag $\{\Delta_I, \Delta_\tau, \Delta_P\}$ where Δ_I and Δ_τ are diagonal 2 × 2 matrices and Δ_P is a full 2 × 2 matrix. For computational convenience the matrix Δ_τ is assumed complex. The *LV*-configuration with the inverse-based controller $C_1(s)$, is no longer robustly stable. μ_{RS} is increased from 0.53 to 4.77 by adding 35 percent time constant uncertainty. The μ-values for the diagonal controller $C_2(s)$ and the μ-optimal controller $C_\mu(s)$ are seen to be only weakly influenced by adding the pole uncertainty. Robust stability is still predicted for the μ-optimal controller.

Gain Uncertainty: The linearized gains of the distillation column may vary tremendously with operating conditions. However, the gains are clearly correlated and it is of crucial importance to take this into account to avoid a hopelessly conservative uncertainty description. If the elements in the steady-state gain matrix (4) were assumed to be independent, the gain matrix would become singular for relative errors in each of the elements exceeding [4]

$$\frac{1}{\gamma^*(G_{LV})} = \frac{1}{138.3} = 0.007 \quad (0.7\%). \qquad (44)$$

Here $\gamma^*(G)$ is the minimized condition number

$$\gamma^*(G) = \min_{D_1, D_2} \gamma(D_1 G D_2) \qquad (45)$$

(D_1 and D_2 are diagonal matrices with real, positive entries.) Physically, we know that the distillation column will not become singular and a more structured uncertainty description is needed. Skogestad and Morari [13] have suggested that for small changes in D/B the variations in the steady-state gains may be captured with *additive uncertainty* on the elements using a *single* perturbation Δ_g. For the *LV*-configuration

$$G_{LV_p}(0) = G_{LV}(0) + r_g \Delta_g \begin{pmatrix} 1 & -1 \\ -\dfrac{D}{B} & \dfrac{D}{B} \end{pmatrix}$$

$$= G_{LV}(0) + \begin{pmatrix} 1 \\ -\dfrac{D}{B} \end{pmatrix} r_g \Delta_g [1 \quad -1] \quad |\Delta_g| < 1. \qquad (46)$$

It is important to note that the additive uncertainty in (46) does not change the input singular vectors $\bar{v}$ and $\underline{v}$. An SVD of the perturbation matrix $\begin{pmatrix} 1 & -1 \\ -1 & 1 \end{pmatrix}$ in (46) yields

$$\bar{v} = \begin{pmatrix} 0.707 \\ -0.707 \end{pmatrix}, \quad \bar{u} = \begin{pmatrix} 0.707 \\ -0.707 \end{pmatrix}.$$

The direction of the input singular vector $\bar{v}$ is the same as that of the nominal plant (4), while the output singular vector $\bar{u}$ is almost perpendicular to that of the nominal plant. This means that this

source of uncertainty is also nice in the sense that it mainly changes the plant at the output.

The values of μ for *RS* and *RP* are shown in Table III for the case of 35 percent gain uncertainty ($r_g = 0.35$). Interestingly enough, it turns out that choosing $r_g = 0.35$, $r_p = 0$ gives very similar results as $r_g = 0$, $r_p = 0.35$ (Fig. 19). Furthermore, combinations of these uncertainties were found to add up approximately in a linear fashion with respect to the value of μ. This confirms that in this case, these two sources of uncertainty (pole and gain uncertainty) have a very similar effect on the plant, and that for computational simplicity we may only want to use one of them. Similar results are found for the *DV*-configuration (Table III).

We conclude that the effect of both the gain uncertainty and the time constant uncertainty is to change the directions at the output of the plant. Furthermore, since output uncertainty may be thought of as a disturbance entering the output of the plant, it is not too surprising that the controllers which were found to yield robust performance in Section IV are not significantly affected by the two additional sources of uncertainty.

VI. DISCUSSION AND CONCLUSION

High-purity distillation columns are inherently ill-conditioned because the product compositions are sensitive to changes in the product flow rates. This may cause performance problems if the uncertainty changes the directionality of the plant. This is the case for the traditional *LV*-configuration, where input uncertainty on each manipulated variable changes the directionality at the input of the plant and makes it impossible to use an inverse-based controller (decoupler). The *DV*-configuration is also ill-conditioned, but the diagonal input uncertainty poses no problem in this case. It is therefore clear that ill-conditioned plants are not necessarily sensitive to diagonal input uncertainty. However, it turns out that the relative gain array [14], defined as RGA = $G(j\omega) \times (G(j\omega)^{-1})^T$ where $\times$ denotes element-by-element multiplication, provides such a measure [15]. We have the following:

- plant with large condition number $\gamma(G)$: performance sensitive to full block input uncertainty;
- plant with large elements in the RGA: performance sensitive to diagonal input uncertainty (and obviously also to full block input uncertainty).

The condition number and the RGA may prove to be useful tools for some applications, but to treat the effect of uncertainty on stability and performance in a rigorous manner for the general case, the structured singular value μ should be used. It is clear that even with a powerful tool like μ the control system design process consists of a sequence of iterative steps involving nonlinear modeling, model reduction, simulation, performance specifications, uncertainty modeling as well as linear analysis and synthesis. In particular, it is nontrivial to arrive at a description of model uncertainty which captures the behavior of the real process and can be treated mathematically. Furthermore, since there are always a number of engineering issues which cannot easily be brought into a formal design procedure like the μ-synthesis procedure, one will probably rarely implement the μ-optimal controller as such. The main strength of μ is therefore that it provides a rigorous basis for analyzing and understanding uncertain linear systems. The μ-optimal controller provides an upper limit on the performance which can be expected by any linear controller for a given plant.

APPENDIX

THE SSV μ AND ITS PROPERTIES

Definition [16]: The function $\mu(M)$, called the structured singular value (SSV), is defined at each frequency such that $\mu^{-1}(M)$ is equal to the *smallest* $\bar{\sigma}(\Delta)$ needed to make $(I + \Delta M)$

TABLE III
VALUES OF μ_{NP}, μ_{RS}, AND μ_{RP} FOR DISTILLATION COLUMN WITH
DIAGONAL INPUT UNCERTAINTY AND EFFECT OF ADDING TIME
CONSTANT UNCERTAINTY (r_τ) AND GAIN UNCERTAINTY (r_g) $(\mu_{NP}$ IS
UNCHANGED)

|		$r_\tau = r_g = 0$		$r_\tau = 0.35$		$r_g = 0.35$	
	μ_{NP}	μ_{RS}	μ_{RP}	μ_{RS}	μ_{RP}	μ_{RS}	μ_{RP}
LV-Configuration							
Inverse Controller,							
$C_1(s), k_1 = 0.7$	0.50	0.53	5.78	4.77	7.50	4.83	7.53
Diagonal PI,							
$C_2(s), k_2 = 2.4$	1.50	1.39	1.70	1.61	1.91	1.47	1.82
Optimal Inverse,							
$C_1(s), k_1 = 0.14$	0.50	0.20	3.29	2.60	4.18	2.62	4.19
"μ-Optimal", $C_\mu(s)$	0.79	0.72	1.06	0.99	1.29	0.87	1.24
DV-Configuration							
Inverse Controller,							
$C_3(s), k_3 = 0.7$	0.50	0.53	0.97	0.83	1.18	0.53	1.07
Diagonal PI, $C_4(s)$	0.81	0.37	1.14	0.85	1.61	0.61	1.45
Optimal Inverse,							
$C_3(s), k_3 = 0.13$	0.50	0.20	0.63	0.47	0.81	0.20	0.73
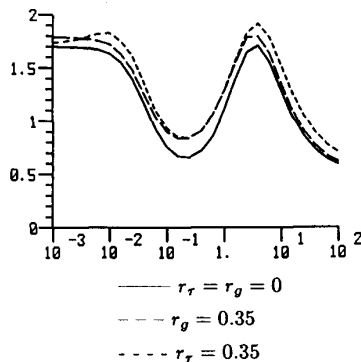
Fig. 19. LV-configuration. μ for RP for diagonal controller $C_2(s)$, $k_2 =$ 0.7. Shows effect of adding gain and time constant uncertainty.

singular, i.e.,

$$\mu^{-1}(M) = \min_\delta \{\delta \mid \det (I + \Delta M) = 0 \quad \text{for some } \Delta, \ \bar{\sigma}(\Delta) \leq \delta(\omega)\}.$$

$$(A\text{-}1)$$

Δ is a *block* diagonal perturbation matrix. $\mu(M)$ depends on the matrix M *and* the structure of the perturbations Δ. Sometimes this is shown explicitly by writing $\mu(M) = \mu_\Delta(M)$.

The above definition is not in itself useful for computing μ since the optimization problem implied by it does not appear to be easily solvable. Fortunately, Doyle [16] has proven several properties of μ which makes it more useful for applications.

Properties of μ [16]:

1) μ is bounded below by the spectral radius and above by the spectral norm:

$$\rho(M) \leq \mu(M) \leq \bar{\sigma}(M) \qquad (A\text{-}2)$$

$\mu(M) = \rho(M)$ in the case $\Delta = \delta I$. $\mu(M) = \bar{\sigma}(M)$ in the case Δ is unstructured, i.e., Δ is a full matrix.

2) Let $\mathfrak{U}$ be the set of all unitary matrices with the same structure as Δ, then

$$\sup_{\mathfrak{U}} \rho(MU) = \mu(M). \qquad (A\text{-}3)$$

This optimization problem is in general not convex.

3) Let $\mathfrak{D}$ be the set of real positive diagonal matrices $D = \text{diag}\ \{d_i I_i\}$ where the size of each block (size of I_i) is equal to the size of the blocks Δ_i. Then for three or fewer blocks

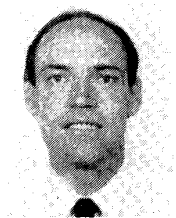$$\inf_{\mathfrak{D}} \bar{\sigma}(DMD^{-1}) = \mu(M). \qquad (A\text{-}4)$$

For four or more blocks, numerical evidence suggests that the left-hand side in (A-4) gives a tight upper bound on $\mu(M)$. A good estimate for the scaling matrix D is found by minimizing $\|DMD^{-1}\|_2$ (the Frobenius norm).

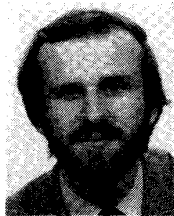4) $\mu(\alpha M) = |\alpha| \mu(M)$, α is a scalar.

REFERENCES

[1] G. Stein, "Beyond singular values and loop shapes," in *Proc. 1985 Amer. Contr. Conf.*, Boston, MA, June 1985.
[2] J. S. Freudenberg and D. P. Looze, "Relations between properties of multivariable feedback systems at different loop-breaking points: Part I," in *Proc. 24th IEEE Conf. Decision Contr.*, Ft. Lauderdale, FL, Dec. 1985.
[3] M. Morari and J. C. Doyle, "A unifying framework for control system design under uncertainty and its implication for chemical process control," in *Proc. CPC III*, Asilomar, CA, Jan. 1986.
[4] S. Skogestad and M. Morari, "Effect of model uncertainty on dynamic resilience," *Chem. Eng. Sci.*, vol. 42, pp. 1765–1780, 1987.
[5] C. N. Nett and V. Manousiouthakis, "Euclidean condition and block relative gain; Connections, conjectures and clarifications," *IEEE Trans. Automat. Contr.*, vol. AC-32, pp. 405–407, 1987.
[6] S. Skogestad and M. Morari, "LV-control of a high-purity distillation column," *Chem. Eng. Sci.*, vol. 43, pp. 33–48, 1988.
[7] F. G. Shinskey, *Distillation Control*, 2nd ed., New York: McGraw-Hill, 1984.

[8] S. Skogestad and M. Morari, "Effect of disturbance directions on closed-loop performance," *Ind. Eng. Chem. Res.,* vol. 26, pp. 2029-2035, 1987.

[9] M. Morari and E. Zafiriou, *Robust Process Control.* Englewood Cliffs, NJ: Prentice Hall.

[10] J. C. Doyle, J. C. Wall, and G. Stein, "Performance and robustness analysis for structured uncertainty," in *Proc. 21st IEEE Conf. Decision Contr.,* Orlando, FL, Dec. 1982.

[11] J. C. Doyle, "Structured uncertainty in control system design," in *Proc. 24th IEEE Conf. Decision Contr.,* Ft. Lauderdale, FL, Dec. 1985.

[12] J. C. Doyle and G. Stein, "Multivariable feedback design: Concepts for a classical/modern synthesis," *IEEE Trans. Automat. Contr.,* vol. AC-26, pp. 4-16, 1981.

[13] S. Skogestad and M. Morari, "Understanding the steady-state behavior of distillation columns," in preparation, 1988.

[14] E. H. Bristol, "On a new measure of interactions for multivariable process control," *IEEE Trans. Automat. Contr.,* vol. AC-11, pp. 133-134, 1966.

[15] S. Skogestad and M. Morari, "Implications of large RGA elements on control performance," *Ind. Eng. Chem. Res.,* vol. 26, pp. 2323-2330, 1987.

[16] J. C. Doyle, "Analysis of feedback systems with structured uncertainties," *IEEE Proc.,* vol. 129, pt. D, pp. 242-250, 1982.

Manfred Morari (A'85-M'87) received the diploma in chemical engineering from the Swiss Federal Institute of Technology in 1974 and the Ph.D. degree from the University of Minnesota in 1977. He was on the faculty of the University of Wisconsin from 1977 to 1983 when he assumed his current position as Professor of Chemical Engineering at the California Institute of Technology, Pasadena. He also held short term positions with Exxon Research & Engineering and ICI. His interests are in the area of process control and design, in particular, robust and decentralized control and the effect of design on operability. He is the principal author of the book *Robust Process Control* (Englewood Cliffs, NJ: Prentice-Hall).

Dr. Morari has received several academic honors including the Donald P. Eckman Award of the American Automatic Control Council in 1980, the Allan P. Colburn Award of the AIChE in 1984, and an NSF Presidential Young Investigator Award also in 1984.
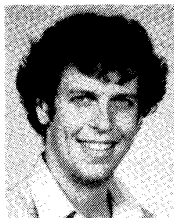
Sigurd Skogestad was born in Norway in 1955. He received the Siv.Ing. degree (Diploma Engineer) in chemical engineering from the Norwegian Institute of Technology (NTH), Trondheim, Norway, in 1978, and the Ph.D. degree in chemical engineering from the California Institute of Technology, Pasadena, in 1987.

During 1979 he served at the Norwegian Defense Research Center, Kjeller, Norway. From 1980 to 1983 he worked with Norsk Hydro in the areas of process design and simulation at their Research Center in Porsgrunn, Norway. He is presently a Professor of Chemical Engineering at NTH, Trondheim. His research interests include robust control, decentralized control, and design and control of chemical plants, in particular, distillation columns.

John C. Doyle received the B.S. and M.S. degrees in electrical engineering from the Massachusetts Institute of Technology, Cambridge, in 1977 and the Ph.D. degree in math from the University of California, Berkeley, in 1984.

He has been a consultant to Honeywell Systems and Research Center since 1976 and an Associate Professor of Electrical Engineering at the California Institute of Technology, Pasadena, since 1986. His research interests include control theory and applications, on which he has published several technical articles.

Dr. Doyle is the recipient of the Hickernell Award, the Eckman Award, the IEEE Control Systems Society Centennial Outstanding Young Engineer Award, and the Bernard Friedman Award. He is an NSF Presidential Young Investigator and an ONR Young Investigator.